On the Orientability of Shapes

Joviša Žunić Paul L. Rosin Lazar Kopanja

***Abstract*— The orientation of a shape is a useful quantity, and has been shown to affect performance of object recognition in the human visual system. Shape orientation has also been used in computer vision to provide a properly oriented frame of reference, which can aid recognition. However, for certain shapes the standard moment based method of orientation estimation fails.**

We introduce as a new shape feature: *shape orientability*, which defines the degree to which a shape has distinct (but not necessarily unique) orientation. A new method is described for measuring shape orientability, and has several desirable properties. In particular, unlike the standard moment based measure of elongation, it is able to differentiate between the varying levels of orientability of n-fold rotationally symmetric shapes. Moreover, the new orientability measure is simple and efficient to compute (for an n-gon we describe an $\mathcal{O}(n)$ algorithm).

***Index Terms*— Shape, orientation, orientability, image processing, early vision.**

I. Introduction

This paper introduces a new shape descriptor, which we call *shape orientability*, whose purpose is to describe the degree to which a shape has distinct (but not necessarily unique) orientation.[1] The computation of a shape's orientation is a common task in the area of computer vision and image processing, being used for example to define a local frame of reference, and helpful for recognition and registration, robot manipulation, etc ([6], [8], [9]). It is also important in human visual perception; for instance, orientable shapes can be matched more quickly than shapes with no distinct axis [17]. Another example is the perceptual difference between a square and a diamond (rotated square) noted by Mach in 1886 [13], which can be explained by their multiple reference frames, i.e. ambiguous orientations [17]. Nevertheless, there remains the problem of determining the reference frame. Many studies have been carried out, and show that in human perception several aspects are involved in this task, such as the shape's axis of symmetry [20] and axis of elongation [21].

There are situations when the orientations of shapes seem to be easily and naturally determined. For example, for shapes that have exactly one axis of symmetry (see Figure 1 (a)) it is reasonable to define the shape orientation by using their symmetry axes. Rectangles and ellipses are naturally oriented by using the longer boundary edge and the longer axis respectively (see Figure 1 (b), (c)). Also, the orientation of some irregular shapes appears reasonably distinct, for example given by some axis of elongation (see Figure 1 (d)). On the other hand, a planar disc could be understood as a shape without orientation.

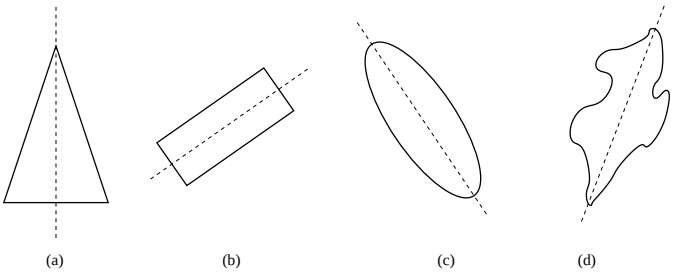

Fig. 1. It is reasonable to say that the orientations of the presented shapes coincide with the dashed lines.

Most situations are somewhere in between. For very non-regular shapes it may be difficult to say what their orientation should be (see Figure 2 (a), (b)). Rotationally symmetric shapes could also have a poorly defined orientation (Figure 2 (c)).

To compute orientation the method based on the axis of the least second moment of inertia ([6], [8], [9]) is the standard one – being widely known and used. It is naturally defined and easy to compute. However, there are situations when the method does not work. For example, the method based on the axis of the least second moment does not specify the orientation of a shape S whose second order central moments satisfy $\overline{m}_{1,1}(S) = 0$ and $\overline{m}_{2,0}(S) = \overline{m}_{0,2}(S)$. There are many shapes (regular and irregular) that satisfy those simple conditions. The main result from [26] says that those conditions are always satisfied by n-fold rotationally symmetric shapes with $n > 2$, for example.

In fact, due to the variety of shapes as well as the diversity of applications there is probably no single method for computing shape orientation that could be efficiently and successfully applicable to all shapes. For that reason, several methods have been developed ([4], [5], [6], [8], [9], [11], [12], [26]). Suitability of those methods strongly depends on the particular situation in which they are applied, as they each have their relative strengths and weaknesses. For instance, one approach reformulates the task using principal component analysis and applies M-estimators to provide more robust orientation estimation, even in the presence of deformations of the shape [1]. Nevertheless, the problems with symmetric shapes remain. The approach used in shape matrices [24] and elsewhere is to base orientation on the maximum radius or diameter. However, for symmetric shapes this will be very sensitive to noise. To overcome deficiencies of existing methods that could only cope with either reflectional symmetry or rotational

J. Žunić is with Computer Science Department, Exeter University, Exeter EX4 4QF, U.K., e-mail: J.Zunic@exeter.ac.uk. (Corresponding Author)

P. L. Rosin is with School of Computer Science, Cardiff University, Cardiff CF24 3AA, U.K., e-mail: Paul.Rosin@cs.cf.ac.uk.

L. Kopanja is with Department of Mathematics and Informatics, Novi Sad University, 21000 Novi Sad, Serbia and Montenegro, e-mail: Kopanjal@yahoo.com.

[1]Note that in this paper we do not mean "orientability" in the topological sense that a two sided surface in $\mathbf{R}^3$ is orientable.

symmetry, Shen and Ip [22], [23] developed a method for estimating the number and orientation of both types of axes of symmetry. However, it requires several tuning parameters, but the computation of many high order generalized complex moments.

As mentioned, rotationally symmetric polygons have a poorly defined orientation. Moreover, even for regular polygons (see Figure 2 (d) and (e)) it is debatable whether they are orientable or not. For instance, is a square an orientable shape? The same question arises not only for any regular n-gon, but also for shapes having several axes of symmetry (Figure 2 (f)), and n-fold ($n > 2$) rotational symmetric shapes. If the answer is "yes, those shapes are orientable", how should the shapes (d), (e), and (f) from Figure 2 be ranked with respect to their orientability? This is another question that is of interest and applicable in the area of shape analysis and shape classification.

Note that the rotation-symmetric and reflective-symmetric shapes appear very often not only in industry (as machine made products) but also in nature (e.g. human face, crystals). The related problems (detection of axes of symmetry, for example) are intensively studied in the literature [2], [7], [14], [18], [23], but some attention has been given to the algebraic structure produced by symmetry operations on planar shapes (see [9] for a short overview).

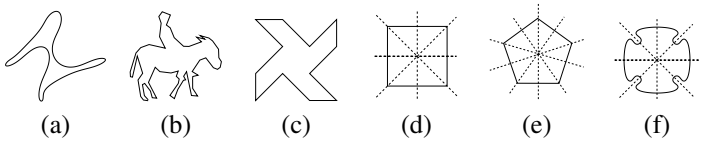

Fig. 2. It is not quite clear what the orientation of the shapes (a), (b), and (c) should be. The dashed lines seem to be reasonable candidates to represent the orientation of the shapes (d), (e), and (f). In the case of the square it is debatable whether the preference should be given to the diagonals or to the vertical (or horizontal) line.

Problems caused by digitization process. The shape orientation problem becomes more complex taking into account that in computer vision and image processing tasks real shapes are replaced with their digitizations. Some specific problems arise when working with digital shapes. Let us mention just two of them:

- Due to the applied digitization process it is possible that some "non-orientable" objects have digitizations whose orientation can be easily computed when the standard method (equation (5)) is applied.
- On the other hand, it is also possible that some orientable objects have digitizations which are not orientable.

The impact of digitization effects on the change in the computed shape orientation is illustrated by the example of a digitized disc and a digitized square. Even though real discs and squares are not "orientable" shapes (see Lemma 1) it could happen that after digitization the obtained discrete point sets have the orientation computable in the standard manner (described in the next section). We demonstrate that the computed orientation could depend strongly on:

(a) shape position with respect to the digitization grid;
(b) applied picture resolution.

The effect of item (a) is illustrated by Figure 3. The same disc is translated into 6 different positions and then digitized. The orientation of the digital disc is not well-defined (in the sense of equation (5)) for positions displayed at Figure 3 (a) and (d), while the digital discs displayed at Figure 3, (b), (c), (e), and (f), have the measured orientations $\varphi = \pi/2$, $\varphi = \pi/2$, $\varphi = \pi/4$, and $\varphi = \pi - \frac{1}{2} \cdot \arctan \frac{3}{4}$, respectively – when equation (5) is applied. We use such a simple example in order to be able to check the results by hand. A higher resolution (or equivalently, a bigger disc is digitized) leads to a larger number of computed orientations which can be obtained if the disc changes its position w.r.t. digitization grid. As an illustration: we have digitized 32 real discs having the radius equal to 10, whose center positions have been chosen randomly. For each choice of center position we have computed the orientation of the obtained digital disc (applying equation (5)). The computed orientations (in the range $[-\pi/2, \pi/2]$)

0.05	0.03	-0.06	-0.59	0.75	-0.01	-0.23	-0.72
0.13	0.00	0.22	-0.57	-0.06	0.29	-0.61	0.63
-0.41	-0.56	-0.29	0.00	0.023	0.14	-0.32	0.11
0.16	-0.01	0.78	-0.74	-0.55	-0.05	0.61	0.25

show that the computed orientation strongly depends on the disc position with respect to the digitization grid.

In Figure 4, the same square is presented in two digital images having different resolutions. In the first case, the standard method does not specify what the orientation of the obtained digital square should be. In the second case, the orientation can be computed easily.

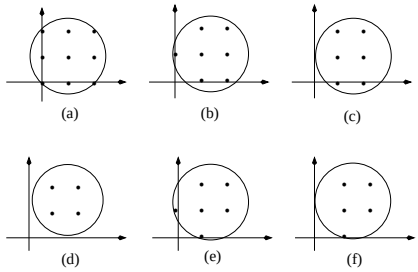

Fig. 3. There are 6 non-isometric digitizations of a disc having the radius $\sqrt{2}$ on a binary picture with resolution 1 (i.e., one pixel per measure unit).

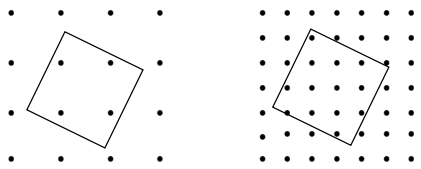

Fig. 4. The same square is presented in digital pictures having different resolutions.

Problems caused by noise effects. Similar problems to the above can be caused by noise effects, as well. For instance, consider a square aligned with the coordinate axes. As mentioned, the standard method does not give any answer as to what the orientation of such a square should be. Adding a single protruding pixel to the boundary can cause the computed orientation to lie anywhere in the range $[-\pi/2, \pi/2]$ depending on its location. As an example, for a 10×10 grid

of pixels adding one pixel to the horizontal or vertical edge gives the following computed orientations:

0.88	1.00	1.14	1.30	1.48	-1.48	-1.30
-1.14	-1.00	-0.88	-0.69	-0.57	-0.43	-0.27
-0.09	0.09	0.27	0.43	0.57	0.69	

Problems caused by the nature of shape. Most of the problems are caused by the nature of the shapes, i.e. because of their inherent inability to be oriented. In Figure 5 (a1), (b1), and (c1) three starfish images are presented. Their boundaries are extracted and presented in Figure 5 (a2), (b2), and (c2). Even though we expected to have the computed orientations for shapes from Figure 5 (a1) (i.e. (a2)) and Figure 5 (b1) (i.e. (b2)) to be very similar (or even coincident) we have obtained (by the standard method) the computed orientations as: -13.7 degrees and 0.4 degrees, respectively. For the shape from Figure 5 (c1) (i.e (c2)) we expected a slightly different orientation. But again, the computed orientation of -36.6 is too far from our expectation.

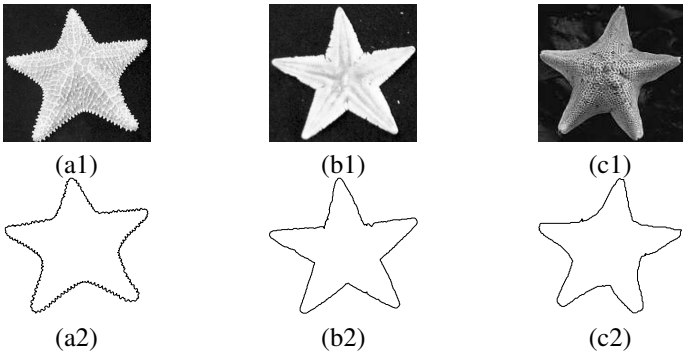

Fig. 5. The differences in estimated orientation of these shapes is due to their deviations from symmetry caused by different viewing angles, natural deformations and variations in the starfish, and noise.

Our conclusion is that the above results for estimated orientation are not realistic simply because the presented shapes cannot be easily oriented – or, in our terms, they should have a low measured orientability.

Problem description. In order to deal with the problems mentioned previously, it is not enough to determine whether the orientation can be computed or not (i.e. does the formula or algorithm used give a result or not?). Rather, it would be more useful to see how stable the solution is. For this purpose we will define *shape orientability* as a new shape descriptor. The main purpose of it is to suggest an answer to the question: *Is the computed orientation just a consequence of digitization or noise effects or is it an inherent property of the considered shape?* We want to describe a shape's orientability as a new shape descriptor that would measure very low orientability values in the cases presented above. As a consequence, a low measure of orientability would suggest that the orientations presented in the previous experiments cannot be accepted as realistic ones – i.e. the reference frame for such shapes should be selected in a more appropriate way or higher quality images must be provided. A second requirement is that we want very elongated ellipses and rectangles to have a very high orientability. Two extreme cases should be circles (with measured orientability equal to 0) and straight line segments (with measured orientability equal to 1).

Organization of the paper. In Section 2 we give a short overview of the most standard method for shape orientation (i.e. the method based on the axis of the least second moment) and characterize some situations when the method is not applicable.

After that, in Section 3, we discuss some intuitive orientability measures that come from the standard definition of shape orientation and we define a new orientability measure. That is the main result of the paper. The defined orientability measure is invariant with respect to similarity transformations, it is normalized to be a number from [0, 1), and it distinguishes a circle as having the lowest possible measured orientability that is equal to 0. Also, there is no shape with measured orientability equal to 1, but shapes having measured orientability arbitrary close to 1 can be constructed. For example, a rectangle with the edge lengths 1 and a has the measured orientability tending to 1 as $a \to \infty$ (see Section 6 and Figure 14).

Section 4 describes an $\mathcal{O}(n)$ procedure for the computation of the new orientability measure of simple n-gons. Some experimental results are shown in Section 5, while Section 6 contains concluding remarks.

II. Standard Method for Computing Orientation

In this section we give a short overview of the method which is mostly used in practice for computing orientation (not the *orientability* computation!) including a lemma that shows that this method cannot be effective when applied to shapes that have several axes of symmetry, for example.

The standard approach defines the orientation by the so called axis of the least second moment ([6], [8]). That is the line which minimizes the integral of the squares of distances of the points (belonging to the shape) to the line. The integral is

$$I(S,\varphi,\rho)=\iint_S r^2(x,y,\varphi,\rho)dxdy \tag{1}$$

where $r(x,y,\varphi,\rho)$ is the perpendicular distance from the point (x,y) to the line given in the form

$$x\cdot\cos\varphi - y\cdot\sin\varphi=\rho.$$

It can be shown that the line that minimizes $I(S,\rho,\varphi)$ passes through the centroid $(x_c(S),y_c(S))$ of the shape S where

$$(x_c(S),y_c(S))=\left(\frac{\iint_S x dxdy}{\iint_S dxdy},\ \frac{\iint_S y dxdy}{\iint_S dxdy}\right).$$

In other words, without loss of generality, we can assume that the origin is placed at the centroid, and so the required line minimizing $I(S,\rho,\varphi)$, passes through the origin – i.e., we can set $\rho=0$. In this way, the shape orientation problem can be reformulated to the problem of determining φ for which the function $F(\varphi,S)$ defined as[2]

$$F(\varphi,S)=I(S,\varphi,\rho=0)=\iint_S (x\cdot\sin\varphi - y\cdot\cos\varphi)^2 dxdy$$

[2]The squared distance of a point (x,y) to the line $X\cdot\cos\varphi - Y\cdot\sin\varphi=0$ is $(x\sin\varphi - y\cos\varphi)^2$.

reaches the minimum. Once again, we assume that the origin coincides with the center of gravity of S.

Further, if the central geometric moments $\overline{m}_{p,q}(S)$ are defined as usual by:

$$\overline{m}_{p,q}(S) = \iint_S (x - x_c(S))^p \cdot (y - y_c(S))^q \, dx \, dy,$$

and if $(x_c(S), y_c(S)) = (0,0)$ then we have

$$F(\varphi, S) = (\sin\varphi)^2 \cdot \overline{m}_{2,0}(S) - \sin(2\cdot\varphi) \cdot \overline{m}_{1,1,}(S) + (\cos\varphi)^2 \cdot \overline{m}_{0,2}(S). \quad (2)$$

The minimum of the function $F(\varphi, S)$ can be computed easily. Setting the first derivative $F'(x, S)$ to zero, we have

$$F'(\varphi, S) = \sin(2\varphi) \cdot (\overline{m}_{2,0}(S) - \overline{m}_{0,2}(S)) - 2 \cdot \cos(2\varphi) \cdot \overline{m}_{1,1}(S) = 0.$$

That easily gives that the required angle φ, but also the angle $\varphi + \pi/2$, satisfies the equation

$$\frac{\sin(2\varphi)}{\cos(2\varphi)} = \frac{2 \cdot \overline{m}_{1,1}(S)}{\overline{m}_{2,0}(S) - \overline{m}_{0,2}(S)}. \quad (3)$$

Consequently, by using (2) and (3), the maximum and minimum of $F(\varphi, S)$ are as follows

$$\max\{F(S,\varphi) \mid \varphi \in [0, 2\pi]\} = \frac{\overline{m}_{2,0}(S) + \overline{m}_{0,2}(S) + \sqrt{4 \cdot (\overline{m}_{1,1}(S))^2 + (\overline{m}_{2,0}(S) - \overline{m}_{0,2}(S))^2}}{2}$$

and

$$\min\{F(S,\varphi) \mid \varphi \in [0, \pi]\} = \frac{\overline{m}_{2,0}(S) + \overline{m}_{0,2}(S) - \sqrt{4 \cdot (\overline{m}_{1,1}(S))^2 + (\overline{m}_{2,0}(S) - \overline{m}_{0,2}(S))^2}}{2}.$$

The ratio between $\max_{\varphi \in [0,\pi)} F(\varphi, S)$ and $\min_{\varphi \in [0,\pi)} F(\varphi, S)$

$$\mathcal{E}(S) = \frac{\max\{F(\varphi, S) \mid \varphi \in [0, 2 \cdot \pi]\}}{\min\{F(\varphi, S) \mid \varphi \in [0, 2 \cdot \pi]\}} \quad (4)$$

is well known as the *elongation* of the shape S, and can also be expressed as

$$\mathcal{E}(S) = \frac{\sqrt{\Phi_2(S)}}{\Phi_1(S)}$$

where $\Phi_1(S)$ and $\Phi_2(S)$ are the first two rotation and translation moment invariants [16].

Let us mention that, when working with digital objects which are actually digitizations of real shapes, the central geometric moments $\overline{m}_{p,q}(S)$ are replaced with their discrete analogue, i.e., with so called *central discrete moments*. Since the digitization on the integer grid $\mathbf{Z}^2$ of a real shape S consists of all pixels whose centers are inside S it is natural to approximate $\overline{m}_{p,q}(S)$ by the central discrete moment $\overline{\mu}_{p,q}(S)$ which is defined as

$$\overline{\mu}_{p,q}(S) = \sum_{(i,j) \in S \cap \mathbf{Z}^2} (i - x_{cd}(S))^p \cdot (j - y_{cd}(S))^q,$$

where $(x_{cd}(S), y_{cd}(S)) = \left(\frac{\sum_{(x,y) \in S \cap \mathbf{Z}^2} x}{\sum_{(x,y) \in S \cap \mathbf{Z}^2} 1}, \frac{\sum_{(x,y) \in S \cap \mathbf{Z}^2} y}{\sum_{(x,y) \in S \cap \mathbf{Z}^2} 1} \right)$ is the centroid of discrete shape $S \cap \mathbf{Z}^2$.

Some details about the efficiency of the approximation $\overline{m}_{p,q}(S) \approx \overline{\mu}_{p,q}(S)$ can be found in [10].

By replacing the geometric moments in (3) with the corresponding discrete moments we obtain the equation

$$\frac{\sin(2\varphi)}{\cos(2\varphi)} = \frac{2 \cdot \overline{\mu}_{1,1}(S)}{\overline{\mu}_{2,0}(S) - \overline{\mu}_{0,2}(S)} \quad (5)$$

which describes the angle φ which is used as an approximate orientation of the shape S, i.e., the angle which is used to describe the orientation of discrete shape $S \cap \mathbf{Z}^2$. It is worth noting that equation (5) can be derived easily if the orientation of the discrete set (a finite number point set) $S \cap \mathbf{Z}^2$ is defined by the line (passing the origin) which minimizes the total sum $\sum_{(i,j) \in S \cap \mathbf{Z}^2} (i \cdot \sin\varphi - j \cdot \cos\varphi)^2)$ of squares of distances of points from $S \cap \mathbf{Z}^2$ to this line.

In other words, the equality (5) can be derived as a consequence when trying to solve the following optimization problem

$$\min \left\{ \sum_{(i,j) \in S \cap \mathbf{Z}^2} (i \cdot \sin\varphi - j \cdot \cos\varphi)^2 \mid \varphi \in [0, \pi] \right\} \quad (6)$$

assuming that the centroid $\left(x_{cd}(S \cap \mathbf{Z}^2),\ y_{cd}(S \cap \mathbf{Z}^2)\right)$ coincides with the origin.

So, the standard method is very simple (in both "real" and "discrete" versions) and it comes from a natural definition of the shape orientation. However, it is not always effective. The next lemma is a direct consequence of Theorem 1 from [26]. It is related to n-fold rotationally symmetric shapes – i.e., such shapes which are identical to themselves after being rotated through any multiple of $\frac{2\pi}{n}$, and it shows that the standard method does not always give a clear result for the shape orientation.

Lemma 1: If a given shape S is n-fold rotationally symmetric, with $n > 2$, then $F(\varphi, S)$ is a constant function.

Remark. Lemma 1 implies that

- $F(\varphi, S) = \frac{1}{2} \cdot (\overline{m}_{2,0}(S) + \overline{m}_{0,2}(S))$ for all $\varphi \in [0, \pi)$;
- $\mathcal{E}(S) = 1$

hold for all n-fold rotationally symmetric shapes with $n > 2$ (trivially, this includes shapes that have more than two axes of symmetry). In other words, the standard method does not tell us what the orientation of shapes from Figure 2(c)-(f) should be, or more generally, what the orientation is for any such rotationally symmetric shape. Also, for all such shapes the measured elongation is 1 (measured in the range $[1, \infty)$ as defined by (4)). So, such shapes have the minimum possible measured elongation – i.e., the same measured elongations as a circle. That is not a desirable property if we would like to understand a circle as the least elongated shape rather than such shapes as Figure 2(c)-(f).

III. Measuring Shape Orientability

In this section we consider what quantity can be used to describe shape orientability – to be used as an inherent shape property.

Intuitively, it can be assumed that shapes with high measured elongation are more orientable than shapes with lower

measured elongation. Thus, the elongation $\mathcal{E}(S)$ (see (4)) can be used to estimate shape orientability. Since $\mathcal{E}(S) \in [1, \infty)$, in order to have the measured orientability between 0 and 1, we can measure the orientability as:

$$1 - \frac{1}{\mathcal{E}(S)}. \tag{7}$$

Several other measures can be derived from the function $F(\varphi, S)$, as well. For example, it is intuitively very clear that a bigger ratio between:

- the area of the region bounded by: the coordinate axes, line $y = \min_{\varphi \in [0,\pi)} F(\varphi, S)$, and line $x = \pi$,

and

- the area of region bounded by: the coordinate axes, line $y = F(\varphi, S)$, and line $x = \pi$,

should indicate a lower shape orientability. So, we can give the following definition.

Definition 1: For a given shape S its orientability $\mathcal{D}_F(S)$ can be measured as

$$\begin{aligned} \mathcal{D}_F(S) &= 1 - \frac{\pi \cdot \min\{F(S,\varphi) \mid \varphi \in [0,\pi)\}}{\int_0^\pi F(S,\varphi) \cdot d\varphi} \\ &= \frac{\sqrt{4 \cdot (\overline{m}_{1,1}(S))^2 \ + \ (\overline{m}_{2,0}(S) - \overline{m}_{0,2}(S))^2}}{\overline{m}_{2,0}(S) + \overline{m}_{0,2}(S)}. \end{aligned}$$

Note 1: Let the principal moments of inertia of a region are denoted by I_1 and I_2. Then another measure of elongation that is found in the literature ([16]) can be expressed as

$$\frac{I_1 - I_2}{I_1 + I_2} = \frac{\sqrt{4 \cdot (\overline{m}_{1,1}(S))^2 \ + \ (\overline{m}_{2,0}(S) - \overline{m}_{0,2}(S))^2}}{\overline{m}_{2,0}(S) + \overline{m}_{0,2}(S)}.$$

That is, although it is derived according to different criteria, it results in the identical formula to $\mathcal{D}_F$.

Obviously, $\mathcal{D}_F(S)$ is easily computable and well-motivated. However, it is clear that all shape orientability measures based on $F(\varphi, S)$ are limited by the result of Lemma 1, i.e., $\mathcal{D}_F(S) = 1 - 1/\mathcal{E}(S) = 0$ for all n-fold rotationally symmetric shapes with $n > 2$. In some situations (applications) a new measure for shape orientability is required that does not have that disadvantage.

We now define such a measure. When dealing with rotationally symmetric shapes that have several axes of symmetry, such shapes do not necessarily have identical measured orientability, as would result when using $1 - 1/\mathcal{E}(S)$ and $\mathcal{D}_F(S)$, for example.

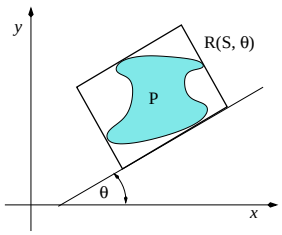

Fig. 6. The rectangle $R(S, \theta)$ is the minimum area rectangle which includes the given shape (shaded area) and whose edges make an angle θ with the coordinate axes.

Definition 2: For a given shape S let $R(S, \theta)$ be the minimal rectangle whose edges make an angle θ with the coordinate axes and which includes S (see Figure 6) and let $\mathbf{A}(R(S, \theta))$ be the area of $R(S, \theta)$. Let

$$\mathcal{A}_{min}(S) \ = \ \min_{\theta \in [0,\pi)} \{ \ \mathbf{A}(R(S,\theta)) \ \}$$

and

$$\mathcal{A}_{max}(S) \ = \ \max_{\theta \in [0,\pi)} \{ \ \mathbf{A}(R(S,\theta)) \ \}.$$

Then, we define the orientability measure $\mathcal{D}(S)$ of the shape S as:

$$\mathcal{D}(S) \ = \ 1 - \frac{\mathcal{A}_{min}(S)}{\mathcal{A}_{max}(S)}.$$

The next theorem describes some desirable properties of $\mathcal{D}(S)$.

Theorem 1: The newly defined measure for shape orientability has the following properties:

a) $\mathcal{D}(S) \in [0, 1)$ for any shape S;
b) A circle has the measured orientability equal to 0;
c) The measured orientability is invariant with respect to similarity transformations.

Proof. **a**) The statement follows easily because $0 < \mathcal{A}_{min}(S) \leq \mathcal{A}_{max}(S)$ holds for any shape S.

b) If S is a circle then $\mathcal{A}_{min}(S) = \mathcal{A}_{max}(S)$ and consequently $\mathcal{D}(S) = 0$.

c) Let $\mathcal{T}$ be a similarity transformation represented by a matrix $\mathbf{T}$. Let a given shape S. The area of the transformed shape $\mathcal{T}(S)$ satisfies $\mathbf{A}(\mathcal{T}(S)) = \det(\mathbf{T}) \cdot \mathbf{A}(S)$, but also $\mathbf{A}(\mathcal{T}(R(S,\theta))) = \det(\mathbf{T}) \cdot \mathbf{A}(R(S,\theta))$, for any angle θ. Thus, $\mathcal{A}_{min}(\mathcal{T}(S)) = \det(\mathbf{T}) \cdot \mathcal{A}_{min}(S)$ and $\mathcal{A}_{max}(\mathcal{T}(S)) = \det(\mathbf{T}) \cdot \mathcal{A}_{max}(S)$ which finally gives $\mathcal{D}(\mathcal{T}(S)) = \mathcal{D}(S)$. □

The new orientability measure of a shape S introduced by Definition 2 is very convenient for numerical computation. A required precision can be reached if $\mathbf{A}(R(S,0))$, $\mathbf{A}(R(S, \frac{\pi}{N}))$, $\mathbf{A}(R(S, 2 \cdot \frac{\pi}{N}))$, ..., $\mathbf{A}(R(S, (N-1) \cdot \frac{\pi}{N}))$, are computed for a sufficiently large N. The exact computation of $\mathcal{D}(S)$ when the measured shape S is a polygon will be described in detail in the next section.

The main objection to $\mathcal{D}(S)$ could be that shapes having the same convex hull have the same measured orientability. That is a disadvantage particularly when $\mathcal{D}(S)$ is used as a shape descriptor in some classification tasks. A slight modification of Definition 2 would ensure that a given non-convex shape does not have the measured orientability equal to the measured orientability of its convex hull. So, we give the next definition.

Definition 3: For a given shape S let $\mathcal{A}_{min}(S)$ and $\mathcal{A}_{max}(S)$ be defined as in Definition 2 and let $\mathbf{A}(S)$ denotes the area of S. Then, for any real number $\alpha \in [0, 1]$ we define the orientability measure $\mathcal{D}_\alpha(S)$ of the shape S as:

$$\mathcal{D}_\alpha(S) \ = \ 1 - \frac{\mathcal{A}_{min}(S) - \alpha \cdot \mathbf{A}(S)}{\mathcal{A}_{max}(S) - \alpha \cdot \mathbf{A}(S)}.$$

Note 2: The orientability measure $\mathcal{D}_\alpha$ also has the desirable properties listed in Theorem 1.

IV. Computation of $\mathcal{D}_\alpha(P)$ when P is a Simple Polygon

From Definition 2 and Definition 3, it is obvious that numerical computation of the orientability $\mathcal{D}_\alpha(S)$ is straightforward.

An arbitrary precision could be reached, although of course higher precision requires higher time complexity.

On the other hand, in particular applications we work with discrete point sets which are discretisations of real shapes. The boundaries of such shapes are necessarily assumed to be polygonal lines – defined in different ways depending on the particular application. In the rest of this section we will assume that considered shapes are bounded by simple polygons and will show that the computation of their orientabilities is possible in linear time with respect to the number of vertices on their boundary.

So, given a simple polygon P, in order to determine $\mathcal{D}_\alpha(P)$ we have to compute the minimum possible area $\mathcal{A}_{min}(P)$ of a rectangle enclosing a given polygon P and the maximum possible area $\mathcal{A}_{max}(P)$ of a rectangle enclosing the polygon P. The construction of a rectangle enclosing P and having the area $\mathcal{A}_{min}(P)$ is already studied in the literature and various approaches exist [3], [15], [25]. The well known result from [3] says that the minimum area rectangle that includes P has one edge that is parallel to an edge of the convex hull of P (denoted as $\mathbf{CH}(P)$). By using this fact and applying the *orthogonal calipers technique* presented in [25], the area $\mathcal{A}_{min}(P)$ can be computed in $\mathcal{O}(n)$ time where n denotes the number of edges of P.

The same statement does not hold for a maximum area rectangle enclosing a given polygon P. A trivial counterexample is a square. Indeed, if P is a square then $\mathbf{CH}(P)$ and the minimum area enclosing rectangle coincide, while the maximum area enclosing rectangle has edges making a $\pi/4$ angle with edges of P. But, we will show that it is still possible to use the orthogonal calipers technique to determine $\mathcal{A}_{max}(P)$.

We briefly present the orthogonal calipers technique. A line L is a *line of support* of P if the interior of P lies completely to one side of L. A pair of vertices is an *antipodal pair* if it admits parallel lines of support. Preparata and Shamos' algorithm [19] generates all antipodal pairs by a procedure which resembles rotating a pair of dynamically adjustable parallel support lines once around the polygon P in order to compute the diameter of P (the diameter of P is defined to be the greatest distance between parallel lines of support of P). This idea is generalized in [25] where two orthogonal pairs of line supports (named *orthogonal calipers*) are formed around the polygon solving several geometric problems. What is important for us is that the same procedure can be used here in order to obtain the intervals

$$[\beta_1, \beta_2], [\beta_2, \beta_3], \ldots, [\beta_{m-1}, \beta_m], [\beta_m, \beta_1 + 2\pi], \quad m \leq n \quad (8)$$

such that:

- Four vertices of an n-gon P (more precisely, four vertices of $\mathbf{CH}(P)$) forming two pairs of antipodal points remain the antipodal points while one of the support lines has the slope $\alpha \in [\beta_i, \beta_{i+1}],\ i = 1, \ldots, m-1$;
- Those four points belong to support lines forming the orthogonal calipers.

Note 3: For any angle $\beta_i \in \{\beta_1, \beta_2, \ldots, \beta_m\} \subset [0,\ 2\pi]$ there is an edge e_i of $\mathbf{CH}(P)$ such that after rotation by the angle β_i the edge e_i becomes parallel to one of coordinate axes.

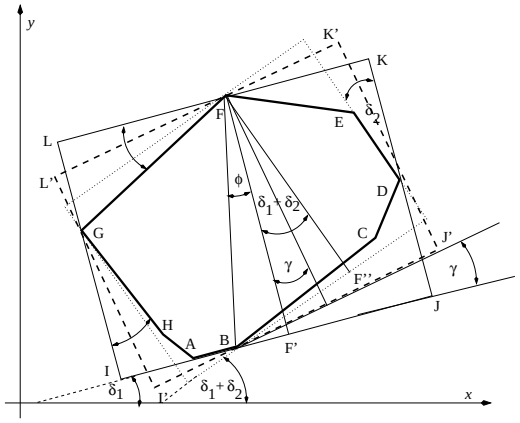

Fig. 7. Illustrating the generation of the orthogonal calipers.

We refer to Figure 7 for an illustration. Let δ_1 be the angle between
the positively oriented x-axis and the edge $[AB]$. Also, let $\delta_2 = \min\{\angle(JBC),\ \angle(KDE),\ \angle(GFL),\ \angle(HGI)\}$ (i.e., δ_2 is the minimum angle between the bounding rectangle and the counterclockwise edges at the antipodal points) – in a situation as in Figure 7, $\delta_2 = \angle(KDE)$.

If the line $l(I, J)$ is chosen to be a support line then B, F and D, G are the antipodal pairs which determine two orthogonal pairs of line supports: $l(I, J), l(L, K)$ and $l(J, K), l(I, L)$. If the support line $l(I, J)$ is rotated into a new position around the vertex B then the pairs B, F and D, G remain antipodal while the rotation γ angle varies from 0 to δ_2 (see Figure 7). (Remark: In the sense of Note 3, we can chose $\beta_1 = \delta_1$, which would imply $\beta_2 = \delta_1 + \delta_2$.)

For $\gamma \in [0, \delta_2]$ the height $d(L'I')$ of the minimal rectangle $L'I'J'K'$ that circumscribes P is

$$d(L'I') \ = \ d(F, F') \cdot \cos(\phi + \gamma) \quad \text{for } \ \gamma \in [0, \delta_2]. \quad (9)$$

and it varies from $d(F, F')$ to $d(F, F'')$, where $d(X, Y)$ is the Euclidean distance between points X and Y. The angle ϕ depends only on the four chosen antipodal points. In the case presented in Figure 7, ϕ can be computed from B, F, D, and G, or equivalently, ϕ is determined by the interval $[\beta_1, \beta_2]$ (by β_1 and β_2, as well).

Analogously, the width $d(I'J')$ of the same rectangle is of the form

$$d(I'J') \ = \ d(G, G'') \cdot \cos(\omega + \gamma) \quad (10)$$

where $\gamma \in [0, \delta_2]$ and ω is a fixed angle which can be computed from δ_1 and δ_2 (i.e., from β_1 and β_2).

Thus, the area of the rectangle $L'I'J'K'$ (i.e., the rectangle $R(P, \gamma)$ in the sense of Definition 2) is

$$\mathbf{A}((R(P, \gamma)) \ =$$
$$d(F, F') \cdot \cos(\phi + \gamma) \cdot d(G, G') \cdot \cos(\omega + \gamma). \quad (11)$$

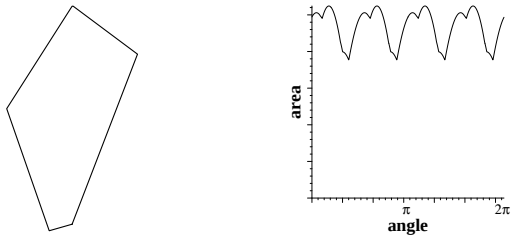

Fig. 8. The graph $\mathbf{A}(R(P,\gamma))$ is shown for a given polygon P. It illustrates that $\mathbf{A}(R(P,\gamma))$ is pairwise of the form (9).

Setting the first derivative equal to zero

$$\frac{d\mathbf{A}(R(P,\phi+\gamma))}{d\gamma} =$$
$$-d(F,F')\cdot d(G,G')\cdot\sin(\phi+\gamma)\cdot\cos(\omega+\gamma)$$
$$-d(F,F')\cdot d(G,G')\cdot\cos(\phi+\gamma)\cdot\sin(\omega+\gamma) =$$
$$-d(F,F')\cdot d(G,G')\cdot\sin(\phi+\omega+2\gamma) \;=\; 0 \qquad (12)$$

we can see that there is at most one point where $\mathbf{A}(R(P,\gamma))$ reaches a local extremum inside the observed interval. More precisely, since $d(L'I') > 0$ and $d(I'J') > 0$ and in accordance with (9) and (10) we have

$$\phi+\gamma \in (-\pi/2,\ \pi/2) \qquad \text{and} \qquad \omega+\gamma \in (-\pi/2, \pi/2)$$

which implies

$$\phi+\omega+2\gamma \in (-\pi, +\pi).$$

Thus, if (12) has a solution in the observed interval then $\phi+\omega+2\gamma$ must be zero. If a solution exists then $\gamma = -\frac{\phi+\omega}{2} \in (0,\beta_2)$.[3]

So, if we repeat the previous analysis for all intervals $[\beta_i,\beta_{i+1}]$, and denote the appearing angles by ϕ_i, ω_i, and γ_i, then we can conclude that $\mathbf{A}(R(P,\gamma))$ $(\gamma \in [0,2\pi))$ reaches its minimum and maximum at some of the endpoints of intervals $[\beta_i,\beta_{i+1}]$ or at one of the solutions γ_i of $\sin(\phi_i+\omega_i+2\gamma_i)=0$ under the assumption that the solution for γ_i belongs in the appropriate interval.

This leads to the following simple procedure can be used for the computation of the newly defined orientability measure for simple polygons $\mathcal{A}_{min}(P)$ and $\mathcal{A}_{max}(P)$.

Note 4: The minimum (maximum) rectangle area value among those computed in **Step 2(c)** and **Step 3** could be reached for several values of γ_i. In other words, a rectangle $R(P,\theta)$ having the area $\mathcal{A}_{min}(P)$ (i.e. $\mathcal{A}_{max}(P)$) may not be determined uniquely. In Figure 11 and Figure 12 below, only one rectangle (corresponding to $\mathcal{A}_{min}(P)$ (i.e. $\mathcal{A}_{max}(P)$)) per displayed shape is presented.

Consequently, we have shown that $\mathcal{D}_\alpha(P)$ can be computed by comparing the values of $\mathbf{A}(R(P,\gamma))$ computed at no more than $\mathcal{O}(n)$ points, where n is the number of vertices of P. Combining this result with the result from [25], which says that all antipodal pairs can be generated in linear time, yields the following theorem.

[3]Further analysis shows that if a local extremum exists it is a local maximum.

Input: A simple n-gon P, a parameter α.

Step 1 Generate all pairs of antipodal pairs which produce the orthogonal calipers of P;

Step 2

(a) Generate all intervals $[\beta_i,\beta_{i+1}]$ defined as in (8);

(b) Generate all angles $\phi_i = \phi_i(\beta_i,\beta_{i+1})$ and $\omega_i = \omega_i(\beta_i,\beta_{i+1})$, for $i=1,2,\ldots,m$;

(c) Compute $\mathbf{A}(R(P,\beta_i))$ for $i=1,2,\ldots,m$.

Step 3 For any $i=1,2,\ldots,m$, such that the solution $\gamma_i = -\frac{\phi_i+\omega_i}{2}$ belongs to the interval (β_i,β_{i+1}) compute $\mathbf{A}(R(P,\gamma_i))$;

Step 4 Set $\mathcal{A}_{min}(P)$ and $\mathcal{A}_{max}(P)$ to the minimum and maximum rectangle area values among those computed in **Step 2(c)** and **Step 3**.

Output: The computed orientability is:

$$\mathcal{D}_\alpha(P) = 1 - \frac{\mathcal{A}_{min}(P) - \alpha\mathbf{A}(P)}{\mathcal{A}_{max}(P) - \alpha\mathbf{A}(P)}.$$

Fig. 9. Algorithm for $\mathcal{D}_\alpha(P)$ computation.

Theorem 2: For a given n-gon P, the orientability $\mathcal{D}_\alpha(P)$ can be computed in $\mathcal{O}(n)$ time.

V. Some Examples

In this section we give some examples of the measured orientability when the new measure is used. The first example (see Figure 10) shows synthetic data, mostly exhibiting both rotational and reflectional symmetries. Theory tells us that $\mathcal{D}_F(S)$ should produce values of zero; in practice quantisation errors have caused non-symmetries, but the values remain close to zero.

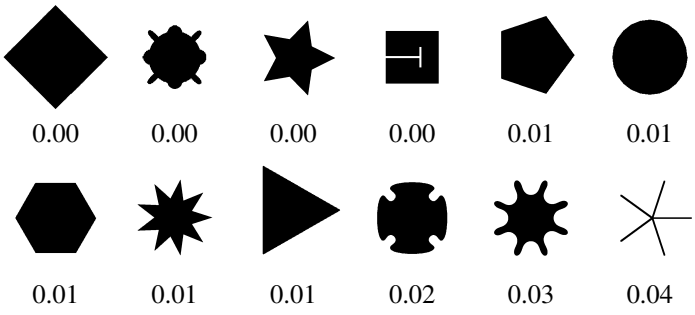

Fig. 10. Synthetic data ordered by orientability using $\mathcal{D}_F(S)$ measure.

The fourth shape in Figure 10 has only one axis of symmetry; nevertheless, since the indentation in the square has a relatively small area it does not substantially affect the values of the moments, and therefore $\mathcal{D}_F(S)$ is approximately zero. Thus, in the context of a shape classification task, all the shapes presented would be assigned to the same group – which is mostly likely to be undesirable.

In contrast to $\mathcal{D}_F(S)$, $\mathcal{D}(S)$ *does* differentiate between the shapes – see Figure 11. Again, according to theory, the second

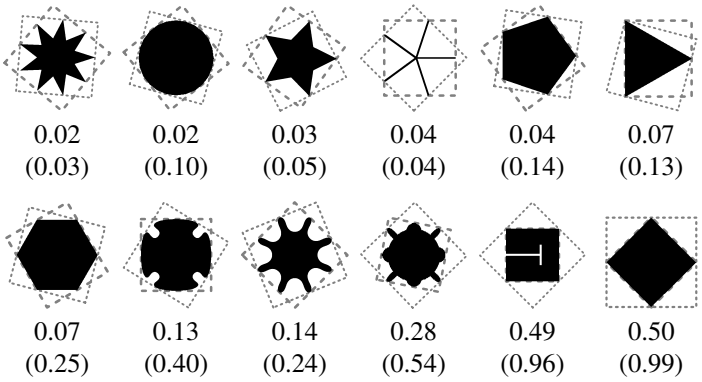

Fig. 11. Synthetic data ordered by orientability using $\mathcal{D}(S)$. The orientabilities measured by $\mathcal{D}_{\alpha=1}(S)$ are given in brackets. The rectangles corresponding to $\mathcal{A}_{min}$ (dashed) and $\mathcal{A}_{max}$ (dotted) are overlaid.

shape in Figure 11 that looks like a circle, but is actually a 24-gon, is assigned a value close to zero. On the other hand, other shapes such as the square are shown by $\mathcal{D}(S)$ to be substantially more orientable than a circle.

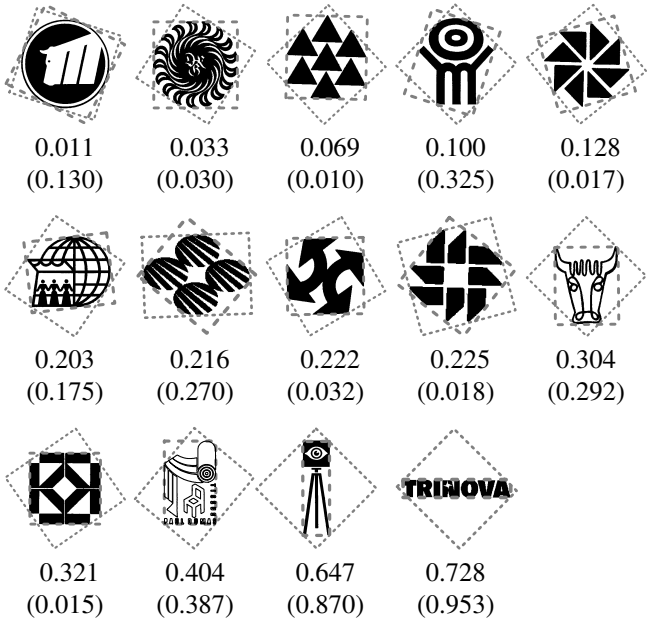

Fig. 12. Trademarks ordered by orientability using $\mathcal{D}(S)$; in brackets are shown $\mathcal{D}_F(S)$ values.

The second set of examples (see Figure 12) consists of some trademarks, and demonstrates the orientability measures for a mixture of shapes, including those with multiple components, asymmetry, internal detail, and naturalistic content. Again, $\mathcal{D}$ behaves as expected, scoring the orientability of the symmetric or roughly symmetric shapes higher than the circular trademark. A very low $\mathcal{D}_F$ orientability and a higher $\mathcal{D}$ orientability could suggest that the measured shape is rotationally symmetric or it has several axes of symmetry (e.g. the middle shape in the second row). In such cases the standard method does not indicate how the shape (in this case a trademark) should be oriented. Thus, since $\mathcal{D}_F$ produces similar near zero values for many shapes it is unable to provide the means to discriminate between them, unlike $\mathcal{D}$. Perhaps a very natural solution for the shape orientation should be one of the axes of symmetry (if any) – for a solution see [14], [18], [23], or more general approaches should be applied [26]. Very elongated shapes (i.e. the last two trademarks) are assigned high orientability values by both measures and the shape orientation is well defined by the standard method.

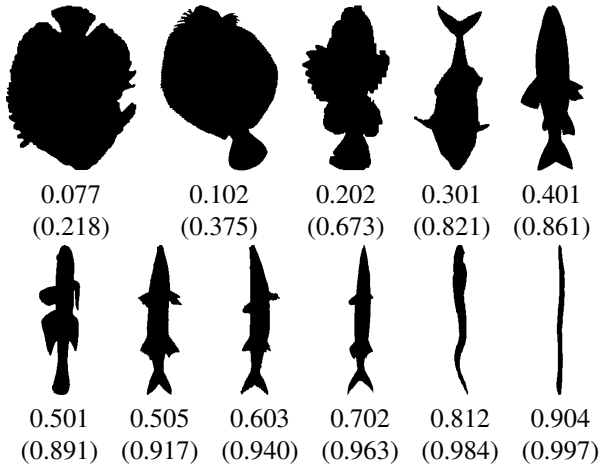

Fig. 13. Fish outlines ordered by orientability using $\mathcal{D}$; in brackets are shown $\mathcal{D}_F$ values.

The final example is presented to show that the orientability measure operates reliably on natural, real world shapes. Figure 13 contains examples of fish from the SQUID database[4]. Both $\mathcal{D}$ and $\mathcal{D}_F$ appear to produce reasonable values.

We also revisit the starfish shapes introduced earlier in the paper and compute the $\mathcal{D}$ measure. For Figure 5 their orientability values are (in order): 0.157, 0.067, and 0.063. Such low values indicate that any estimate of orientation is likely to be unstable

We did not discuss the effects of digitizations on the computation of $\mathcal{D}(S)$. It is clear that $\mathcal{D}(S)$ is well defined for any compact shape S and consequently, a high enough picture resolution will provide the required precision in $\mathcal{D}(S)$ computation. The effects of quantisation on $\mathcal{D}(S)$ are demonstrated for digital circles in Figure 14. The graph shows that for small radius values $\mathcal{D}(S) = 0.5$, since the digital circle is equivalent to a square. As the circle radius increases the measured $\mathcal{D}(S)$ approaches the true value of zero.

It should be noted that the computation overheads of calculating $\mathcal{D}$ are low. For the results shown in this paper the typical

[4]The SQUID database and an online demo is available from Surrey University at http://www.ee.surrey.ac.uk/Research/VSSP/imagedb/.

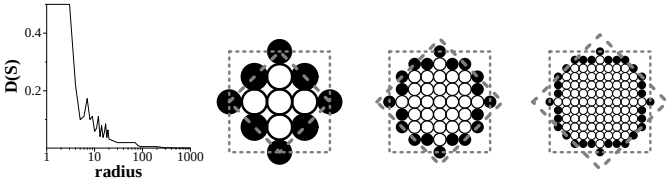

Fig. 14. The graph shows the effect of quantisation on $\mathcal{D}(S)$. Some examples of digitised circles (with radii 2, 4, and 6) centred at the origin are given. Their maximum and minimum area rectangles are displayed as well.

run times on the shapes, which mostly contained around 500-1500 points, were less than 0.1 ms on a 2.0 GHz Pentium 4 (including I/O and the determination of the convex hull).

VI. Concluding Remarks

In this paper we define shape orientability as a new shape descriptor. We also discuss some approaches (those coming naturally from the definition of shape orientation) for measuring shape orientability and define a new measure. The purpose of such a measure is to give an answer as to whether the computed orientation of a shape is an inherent property of the considered shape, or whether it comes from artifacts caused by the digitization process or by noise, for example. The measure can be useful when applied to shapes whose measured orientation changes even under slight deformations [1].

The shape orientability measured by the method presented here is a number from $[0, 1)$ and it is invariant with respect to similarity transformations. A disc has the measured orientability equal to zero – which is the theoretical minimum. There is no shape with a measured orientability equal to 1. Even in cases where there is no doubt what the orientation should be, e.g. an elongated rectangle, the measured orientability is not 1. Precisely, the new measure says that if the ratio between the length of the longer edge and the length of the shorter edge increases then the orientability for rectangles increases as well. That is a desirable property. In the limit case, if this ratio tends to infinity, it is natural to expect that the measured orientability tends to 1 and we could say that a straight line segment is a perfectly oriented shape. That is exactly what happens – see the item **(a)** in Appendix. Another desirable property is that shapes with several axes of symmetry and rotationally symmetric shapes could have non-zero measured orientability – see the item **(b)** in Appendix.

Acknowledgments

The authors would like to Aditya Vailaya for providing the trademark database, and Farzin Mokhtarian for the SQUID database.

References

[1] J. Cortadellas, J. Amat, F. de la Torre, "Robust Normalization of Silhouettes for Recognition Application," *Patt. Rec. Lett.,* Vol. 25, pp. 591-601, 2004.

[2] S. Derrode and F. Ghorbel "Shape Analysis and Symmetry Detection in Gray-Level Objects Using the Analytical Fourier-Mellin Representation," *Signal Processing,* Vol. 84, pp. 25-39, 2004.

[3] H. Freeman, R. Shapira, "Determining the Minimum-Area Encasing Rectangle for an Arbitrary Closed Curve," *Comm. of the ACM,* Vol. 18, pp. 409-413, 1975.

[4] V. H. S. Ha and J. M. F. Moura, "Efficient Shape Orientation," Proceedings of IEEE Conference on Image Processing, Vol. 1, pp. 225-228, 2003.

[5] V.H.S. Ha and J.M.F. Moura, "Robust Reorientation of 2D Shapes Using the Orientation Indicator Index," Proceedings of ICASSP, pp. 777–780, 2005.

[6] B.K.P. Horn, *Robot Vision,* MIT Press, Cambridge, MA, 1986.

[7] A. Imiya, T. Ueno, and I. Fermin, "Discovery of Symmetry by Voting Method," *Engineering Application of Artificial Intelligence,* Vol. 15, pp. 161-168, 2002.

[8] R. Jain, R. Kasturi, B.G. Schunck, *Machine Vision,* McGraw-Hill, New York, 1995.

[9] R. Klette, A. Rosenfeld *Digital Geometry,* Morgan Kaufmann, San Francisco, 2004.

[10] R. Klette, J. Žunić, "Digital approximation of moments of convex regions," *Graphical Models and Image Processing,* Vol. 61, pp. 274-298, 1999.

[11] J.-C. Lin, "Universal Principal Axes: An Easy-to-Construct Tool Useful in Defining Shape Orientations for Almost Every Kind of Shape," *Pattern Recognition,* Vol. 26, No. 4, pp. 485–493, 1993.

[12] J.-C. Lin, "The Family of Universal Axes," *Patt. Rec.,* Vol. 29, pp. 477-485, 1996.

[13] E. Mach, *The Analysis of Sensations (Beiträge zur Analyse der Empfindungen),* Routledge, London, 1996.

[14] G. Marola, "On the Detection of Axes of Symmetry of Symmetric and Almost Symmetric Planar Images," *IEEE Trans. PAMI,* Vol. 11, No. 6, pp. 104-108, 1989.

[15] R.R. Martin, P.C. Stephenson, "Putting Objects into Boxes," *Computer Aided Design,* Vol.20, pp. 506-514, 1988.

[16] R. Mukundan, K. R. Ramakrishnan, *Moment Functions in Image Analysis – Theory and Applications,* World Scientific, Singapore, 1998.

[17] S.E. Palmer, *Vision Science: Photons to Phenomenology,* MIT Press, 1999.

[18] V. Shiv Naga Prasad and B. Yegnanarayana, "Finding Axes of Symmetry from Potential Fields," *IEEE Trans. Image Processing,* Vol. 13, No. 12, pp. 1559-1556, 2004.

[19] F.P. Preparata and M.I. Shamos, *Computational Geometry,* Springer-Verlag, 1985.

[20] P.T. Quilan and G.W. Humphreys, "Perceptual frames of reference and two-dimensional shape recognition," *Perception,* Vol. 22, pp. 1343-1364, 1993.

[21] A.B. Sekuler, "Axis of elongation can determine reference frames for object perception," *Canadian J. of Experimental Psychology,* Vol. 50, No. 3, pp. 270-279, 1996.

[22] D. Shen, H.H.S. Ip, "Generalized Affine Invariant Normalization," *IEEE Trans. PAMI,* Vol. 19, No. 5, pp. 431-440, 1997.

[23] D. Shen, H.H.S. Ip, K.K.T. Cheung, and E.K. Teoh, "Symmetry Detection by Generalized Complex (GC) Moments: A Close-Form Solution," *IEEE Trans. PAMI,* Vol. 21, No. 5, pp. 466–476, 1999.

[24] A. Taza and C.Y. Suen, "Discrimination of Planar Shapes Using Shape Matrices," *IEEE Trans. System, Man and Cybernetics,* Vol. 19, No. 5, pp. 1281–1289, 1989.

[25] G.T. Toussaint, "Solving geometric problems with the rotating calipers," *Proc. IEEE MELECON '83*, pages A10.02/1–4, 1983.

[26] W.H. Tsai, S.L. Chou, "Detection of Generalized Principal Axes in Rotationally Symmetric Shapes," *Patt. Rec.,* Vol. 24, pp. 95-104, 1991.

Appendix

(a) A rectangle $P(a)$ having edge lengths equal to 1 and $a > 1$ is presented in Figure 15. Applying the results from Section 4 we derive $\mathbf{A}(R(P(a), \gamma)) = (a^2+1) \cdot \cos(\gamma - \arctan(a)) \cdot \cos(\gamma - (\frac{\pi}{2} - \arctan(a)))$ which gives $\mathcal{A}_{max}(P(a)) = \frac{(a+1)^2}{2}$. Of course, $\mathcal{A}_{min}(P(a)) = a$ and consequently (by Definition 2)

$$\mathcal{D}(P(a)) \;=\; \frac{a^2+1}{a^2+2a+1} \;\to\; 1, \qquad \text{as} \quad a \to \infty.$$

(b) A regular $4n$-gon P_{4n} has the measured orientability $\mathcal{D}(P_{4n})$ equal to $\mathcal{D}(P_{4n}) = 1 - \frac{4\cos\frac{\pi}{4n}}{4} = 1 - \cos\frac{\pi}{4n}$. Obviously, $\lim_{n\to\infty} \mathcal{D}(P_{4n}) = 0$, as expected.

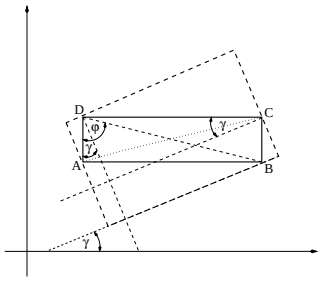

Fig. 15. The orientability $\mathcal{D}(P)$ of a rectangle P having one edge length equal to 1 and another equal to $a > 1$ is $\mathcal{D}(P) = (a^2 + 1)/(a + 1)^2$ and tends to 1 as $a \to \infty$.